Aurora A kinase activity influences calcium signaling in kidney cells

Olga V. Plotnikova, Elena N. Pugacheva, and Erica A. Golemis

Department of Developmental Therapeutics, Fox Chase Cancer Center, Philadelphia, PA 19111

Most studies of Aurora A (AurA) describe it as a mitotic centrosomal kinase. However, we and others have recently identified AurA functions as diverse as control of ciliary resorption, cell differentiation, and cell polarity control in interphase cells. In these activities, AurA is transiently activated by noncanonical signals, including Ca^{2+}-dependent calmodulin binding. These and other observations suggested that AurA might be involved in pathological conditions, such as polycystic kidney disease (PKD). In this paper, we show that AurA is abundant in normal kidney tissue but is also abnormally expressed and activated in cells lining PKD-associated renal cysts. PKD arises from mutations in the *PKD1* or *PKD2* genes, encoding polycystins 1 and 2 (PC1 and PC2). AurA binds, phosphorylates, and reduces the activity of PC2, a Ca^{2+}-permeable nonselective cation channel and, thus, limits the amplitude of Ca^{2+} release from the endoplasmic reticulum. These and other findings suggest AurA may be a relevant new biomarker or target in the therapy of PKD.

Introduction

The Aurora A (AurA) kinase is overexpressed in a high percentage of tumors arising in breast, colon, ovary, and other tissues (Bischoff et al., 1998; Zhou et al., 1998; Tanaka et al., 1999; Tanner et al., 2000; Goepfert et al., 2002) and functions as an oncogene when exogenously expressed in cell line models for cancer development (Tatsuka et al., 1998; Meraldi et al., 2002; Anand et al., 2003; Zhang et al., 2004). In normal cells, one important function of AurA is as a centrosomally localized regulator of entry into and passage through mitosis (Marumoto et al., 2005; Pugacheva and Golemis, 2006); defects in these roles likely explain the supernumerary centrosomes and aneuploidy that characterize tumor cells with overexpressed AurA. Many studies of AurA performed in mammals and model organisms have shown that AurA kinase activity increases sharply at the G2/M boundary and is highest through M phase in normal cells based on interactions with partner proteins, including TPX2, NEDD9/HEF1, and others (Bayliss et al., 2003; Pugacheva and Golemis, 2005; Hutterer et al., 2006). Activated AurA detected in interphase cancer cells was initially attributed to a pathological disease state, unreflective of the role for AurA in normal cells. However, convergence of several lines of investigation has begun to greatly extend known roles for AurA.

Initial evidence for nonmitotic AurA functions arose from a study of the *Chlamydomonas reinhardtii* aurora protein kinase, a distant orthologue of AurA in the green algae *C. reinhardtii* (Pan et al., 2004). This work revealed that *C. reinhardtii* aurora protein kinase is activated and regulates resorption of the flagella in response to cues for mating or environmental ionic stress, rather than cell cycle cues. Subsequently, our group established that serum growth factors induce AurA activation at the basal body of the cell cilium (a structure analogous to the flagellum) in noncycling G0/G1 mammalian cells causing AurA- and NEDD9-dependent ciliary resorption (Pugacheva et al., 2007). We further showed that release of Ca^{2+} from the ER to the cytoplasm transiently activated AurA, based on induced direct Ca^{2+}-calmodulin (CaM) binding to AurA (Plotnikova et al., 2010). Independently, other groups have found that atypical PKC activates AurA, allowing AurA to phosphorylate NDEL1 and promote microtubule remodeling during neurite extension (Mori et al., 2009). AurA has also been found to directly phosphorylate Par-6, which together with atypical PKC and Par-3 regulates asymmetric cell division and cell polarity (Ogawa et al., 2009; Yamada et al., 2010). These nonmitotic activities of AurA likely also contribute to deregulation of growth in tumor cells overexpressing AurA. For example, interphase-active AurA

Correspondence to Erica A. Golemis: EA_Golemis@fccc.edu

Abbreviations used in this paper: ADPKD, autosomal dominant PKD; AUC, area under curve; AurA, Aurora A; AVP, arginine vasopressin; CaM, calmodulin; IC, inhibitory concentration; PKD, polycystic kidney disease.

The Rockefeller University Press $30.00
J. Cell Biol. Vol. 193 No. 6 1021–1032
www.jcb.org/cgi/doi/10.1083/jcb.201012061

phosphorylates and promotes the activity of the RalA GTPase, an epidermal growth factor receptor/Ras effector important in many cancers (Wu et al., 2005). Loss of cilia associated with high level AurA expression would indirectly impact the functionality of the cilia-dependent and cancer-relevant signaling cascades, such as those involving Hedgehog (Wong et al., 2009).

Pathological conditions of the kidney include renal cell carcinoma, which has been linked to elevated AurA expression (Kurahashi et al., 2007). However, beyond high expression in kidney tumors, AurA (Kurahashi et al., 2007) and its partner NEDD9 (Law et al., 1996; Pugacheva and Golemis, 2005, 2006) have been predicted to be abundant in normal kidneys. Interestingly, formation of renal cysts is very strongly linked to defects in planar cell polarity control (Fischer et al., 2006; Bacallao and McNeill, 2009), and the changes in Ca^{2+} signaling induced by autosomal dominant polycystic kidney disease (PKD; ADPKD)–associated mutations in the *PKD1* and *PKD2* genes, encoding the PC1 transmembrane flow receptor and the PC2 calcium channel (Hanaoka et al., 2000; Wilson, 2004; Pan et al., 2005; Benzing and Walz, 2006). Interestingly, an antibody cross-reactive with NEDD9 and its paralogue BCAR1/p130Cas has been reported as detecting one of these proteins in a complex with PC1 (Geng et al., 2000). NEDD9 binds directly to the differentiation regulatory protein Id2 (Law et al., 1999), which in turn has been reported to bind directly to PC2 and mediate proliferative signals in PKD (Li et al., 2005). Cumulatively, these studies led us to hypothesize that changes in AurA and/or NEDD9 expression or activity might have a role in signaling processes associated with development of renal cysts.

Based on these and other studies, we have investigated AurA in kidney signaling relevant to cystogenesis. Our work demonstrates that AurA is abundant and frequently active in normal renal tissue and hyperactivated in early renal cysts associated with PKD. We show that low concentrations of drugs that inhibit AurA activity augment basal intracellular Ca^{2+} levels in renal cells and PC2-dependent Ca^{2+} release. We also find that AurA directly binds and phosphorylates PC2, which may provide a mechanism by which AurA inhibition limits PC2 Ca^{2+} channel activity. ADPKD affects as many as 1 in 500 individuals and currently has few viable treatment options. The results described here may suggest potential clinical applications of AurA and its inhibitors in better diagnosing or treating this serious disease.

Results

Abundant AurA expression and activity in normal kidney tissue and cells and in renal cysts

If AurA has in vivo, noncell cycle function relevant to PKD, AurA should be detectable and potentially active in nondividing renal tissue. Immunohistochemical analysis of primary human kidney specimens readily detected AurA in multiple substructures (Fig. 1 a and Fig. S1 a). AurA was most concentrated in cells of the proximal and particularly distal convoluted tubules and in the collecting ducts. AurA was not detectable in the glomerulus or in the loops of Henle. This expression pattern is similar to that previously reported for PC2, which is also abundant in the convoluted tubules and collecting ducts, although PC2 is also abundant in the loops of Henle (Foggensteiner et al., 2000). AurA staining was generally detectable in the cytoplasm but also intensely concentrated in the nucleus of some cells, with the greatest number of nuclear-staining cells associated with the distal convoluted tubules. Suggestively, a subset of these AurA-positive structures also stained positively for T^{288}-phospho–AurA (phAurA), indicating activity across adjacent groups of nonmitotic cells (Fig. 1 b and Fig. S1 a); again, the most intense staining was associated with distal convoluted tubules and collecting ducts. As further confirmation, we also examined AurA and phAurA expression in mouse renal tissue (Fig. 1, c and d; and Fig. S1 a) and found a similar expression and activation pattern.

AurA is typically described as solely localized to the centrosome or centrosomally derived ciliary basal body and otherwise hard to detect in noncycling normal mammalian cells. In this context, the fact that cancerous cells with overexpressed AurA have an extensive diffuse pool of cytoplasmic AurA is thought to support the interaction of AurA with substrates with which it does not normally associate (discussed in Pugacheva and Golemis, 2006). However, we find AurA is intrinsically abundant in HK-2 cells, a well-differentiated cell line derived from the proximal tubules of the human kidney (Ryan et al., 1994), in primary nontransformed human ovarian surface epithelial cells (Fig. 2 a) and in noncycling primary mouse kidney cells (Fig. S1 b). Moreover, siRNA depletion experiments of HK-2 cells followed by detection with two different antibodies to AurA (Fig. 2 b and not depicted) indicated the presence of a significant cytoplasmic pool of AurA in interphase HK-2 cells in addition to the anticipated concentrated pool of AurA at centrosomes.

We next investigated whether AurA expression, localization, or activation was specifically altered in the context of PKD. Examination of eight primary cysts derived from eight patients with PKD (Fig. 2 c) revealed prominent AurA staining specifically within the epithelial cells lining the cyst but not the fibrotic tissue. This was particularly noticeable in small and midsized cysts and in areas of hyperproliferative epithelial cells adjacent to cysts and was accompanied by a strong T^{288}-phAurA signal, indicating kinase activation.

AurA negatively regulates basal cellular Ca^{2+} levels and PC2-dependent Ca^{2+} channel activity

We have shown that Ca^{2+} transiently activates AurA (Plotnikova et al., 2010), and our data indicate that in the abnormal Ca^{2+} signaling environment associated with PKD renal cysts (Anyatonwu and Ehrlich, 2004), AurA expression is enhanced. We hypothesized that AurA might reciprocally influence cellular Ca^{2+} levels in a typical signaling feedback circuit (Sneppen et al., 2010). Indeed, treatment of HK-2 and LLCPK1 kidney cells with the AurA inhibitor PHA-680632 for 3 h significantly increased basal levels of Ca^{2+}, based on measurement of the fluorescence of the cytoplasmic Ca^{2+}-binding dye Fluo-4 (Fig. 3 a; Cai et al., 2004). Similar results were obtained after depletion of AurA by siRNA in LLCPK1 cells (Fig. 3 b) and HEK293 cells (not depicted).

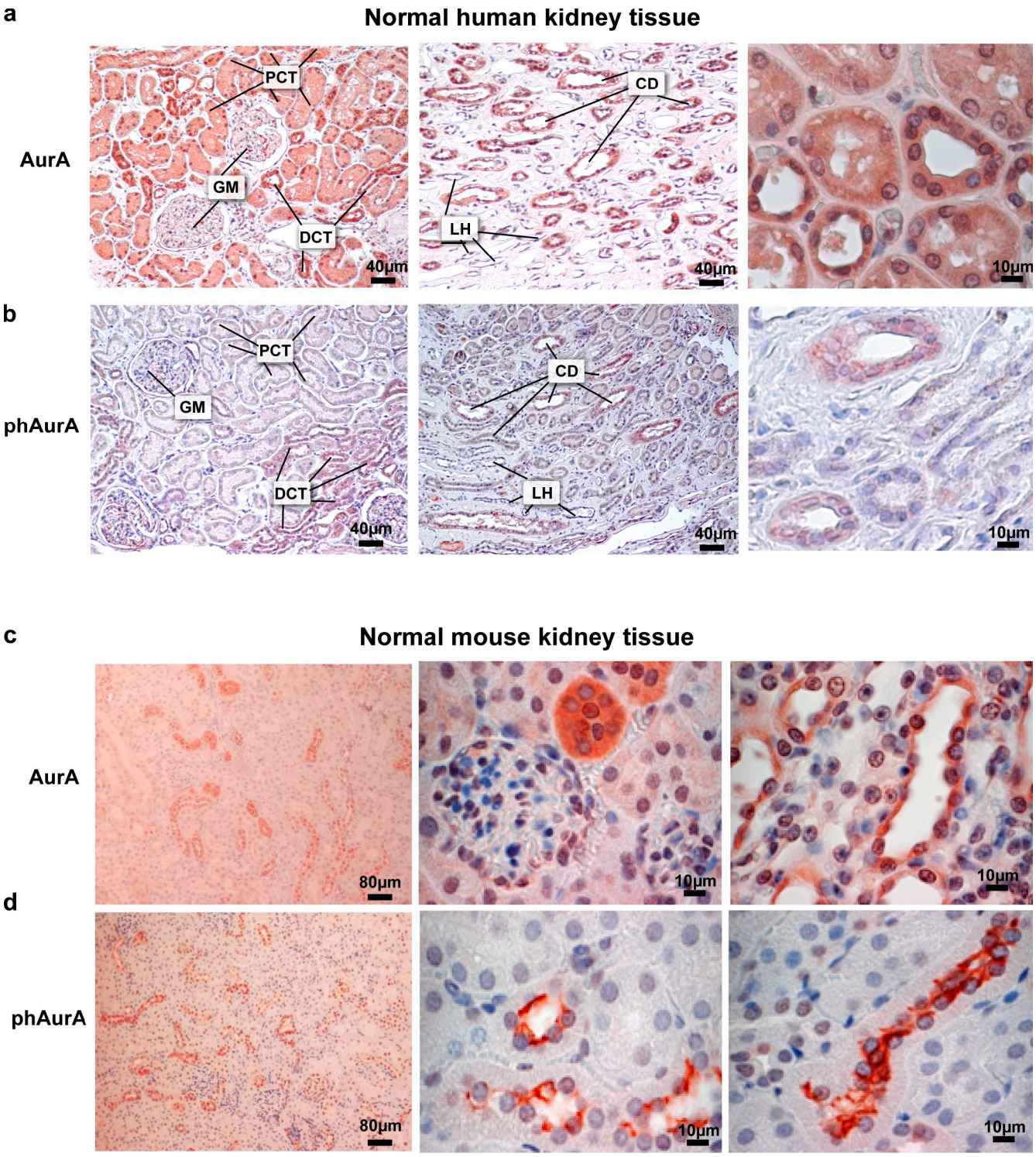

Figure 1. **Abundant AurA expression and activity in normal kidney tissue and cells.** (a and b). Immunohistochemical visualization of endogenous total AurA (a) or phAurA (b) in normal human kidney tissue. Typical fields from the cortical (left) and medullary regions (center) are shown. PCT, proximal convoluted tubules; DCT, distal convoluted tubules; CD, collecting ducts; LH, thin segments of Loops of Henle; GM, glomerulus. (c and d) Immunohistochemical visualization of endogenous AurA (c) or phAurA (d) in normal mouse kidney tissue. (right) Sections stained with antibody to AurA preincubated with blocking peptide and, for phAurA, negative control IgG.

The PC2 Ca^{2+} channel is abundant and active in kidney cells. In PKD, PC2 has abnormally reduced function as a result of direct mutation or mutation of its upstream partner PC1 (with which it heterodimerizes at cilia), resulting in abnormal Ca^{2+} homeostasis. Cell lines lacking PC2 have reduced basal Ca^{2+} level (Qian et al., 2003; Geng et al., 2008). To test whether AurA might modulate intracellular Ca^{2+} level through regulation of the PC2 calcium channel, we used $Pkd2^{+/-}$ and $Pkd2^{-/-}$ kidney cell lines derived from mutant mice (Grimm et al., 2003; Geng et al., 2008). $Pkd2^{-/-}$ cells have a reduced level of basal

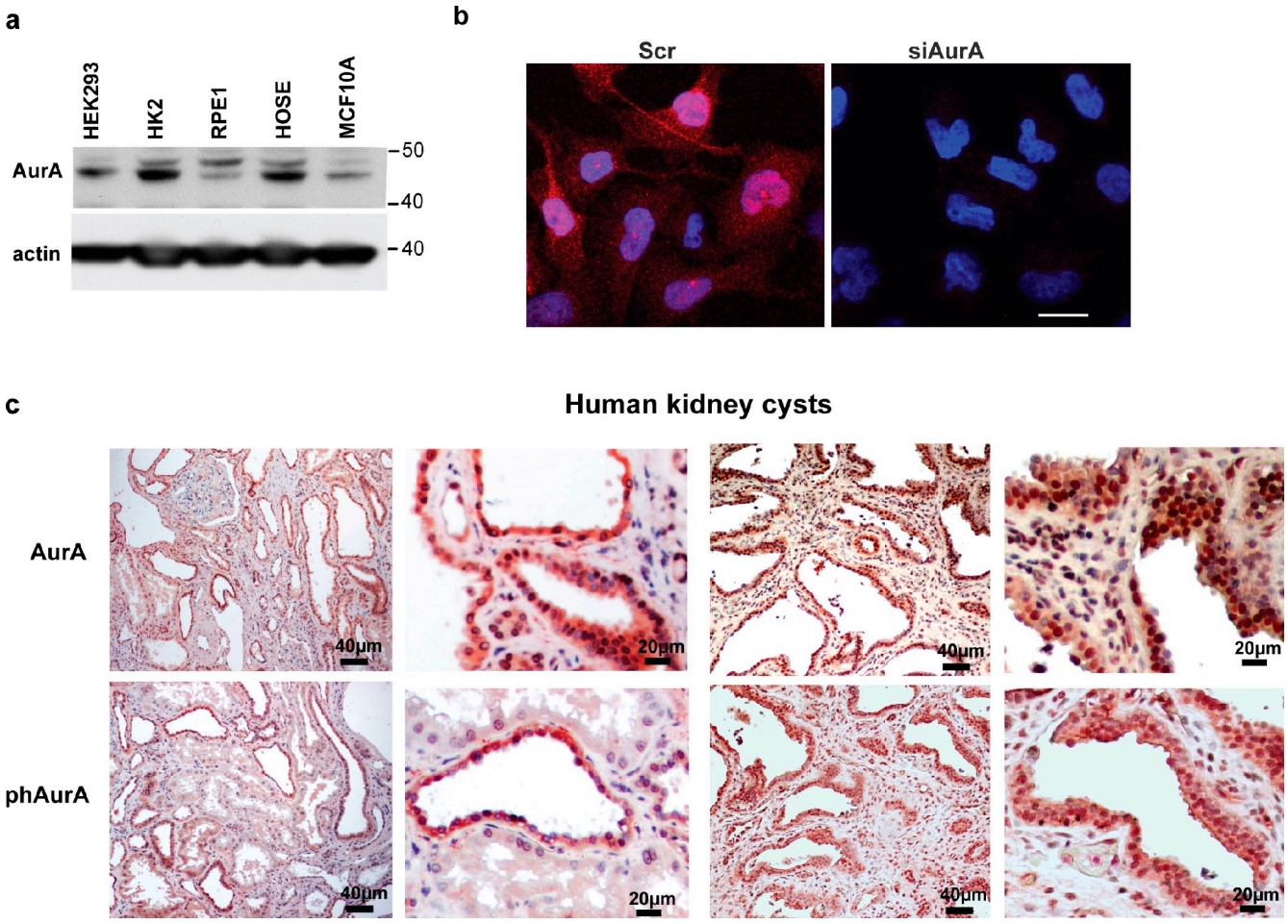

Figure 2. **Abnormal AurA expression and activity in renal cysts.** (a) Western blot analysis of total AurA levels in human cells: HEK293, human embryonic kidney cells; HK-2, adult human kidney epithelial cells; RPE1, immortalized retinal pigment epithelial cells; HOSE, primary human ovarian surface epithelial cells; MCF10A, immortalized mammary epithelial cells. For all experiments, β-actin was used as a loading control. (b) Immunofluorescence of HK-2 cells treated with siRNA to deplete AurA (siAurA) or with control scrambled siRNA (Scr). Bar, 10 µm. (c) Immunohistochemical detection of AurA and phAurA in renal cysts from PKD patients. Epithelial cells lining cysts and cyst-associated areas of hyperproliferative epithelial cells, but not cyst-associated fibrotic tissue, consistently demonstrate strong staining. Molecular masses are given in kilodaltons.

Ca^{2+} compared with $Pkd2^{+/-}$ cells as previously described (Fig. 3 c; Geng et al., 2008). Treatment with the AurA inhibitor PHA-680632 significantly increased intracellular Ca^{2+} levels in both $Pkd2^{+/-}$ and $Pkd2^{-/-}$ cells but was less active in $Pkd2^{-/-}$ cells (Fig. 3 c), whereas the levels of AurA were equivalent in both $Pkd2^{+/-}$ and $Pkd2^{-/-}$ cell lines (Fig. S1 b). Those data implied that AurA influenced basal Ca^{2+} in a process at least partially dependent on intact PC2. We also further demonstrated that PHA-680632 did increase basal Ca^{2+} level in human kidney cell lines with a mutated PKD1 gene but an intact PKD2 gene (Fig. 3 d; Loghman-Adham et al., 2003), as would be expected if the AurA target were downstream of PKD1.

To more directly test whether AurA regulates the PC2 Ca^{2+} channel, we transiently transfected HEK293 cells with PC2 together with RFP-AurA or an RFP negative control and measured fluorescence of the cytoplasmic Ca^{2+}-binding dye Fluo-4 after arginine vasopressin (AVP) treatment, comparing the amplitude and duration of Ca^{2+} release (Fig. 3, e and f; and Fig. S3 a). Cotransfected RFP-AurA reduced the amplitude of the Fluo-4 signal to 50% of that in control-transfected cells. An equivalent response was seen in cells in which histamine was used to induce PC2 channel activity (Fig. S1, c–e). Reciprocally, treatment of PC2-transfected HEK293 cells with the AurA inhibitor PHA-680632 (Soncini et al., 2006) significantly enhanced the amplitude of release (Fig. 3, g and h; and Fig. S3 b). Similar results were obtained using HK-2 cells stably overexpressing PC2 (Fig. S1, f–h) and in cells treated with a separate small molecule inhibitor of AurA, C1368 (Fig. S1, i–k). In PC2-overexpressing HK-2 cells with AurA depleted by siRNA, AVP-induced Ca^{2+} release was significantly increased to a degree comparable with that seen with treatment with AurA inhibitory drugs (Fig. 3, i and j; Fig. S1 l; and Fig. S3 c). Together, these data strongly implicated AurA as a regulator of PC2 channel activity.

PHA-680632 enhances PC2 activity at low inhibitory concentration (IC) values

Given that one consequence of mutations in PKD1 is to reduce PC2 activation (Nauli et al., 2003), if AurA inhibition enhances PC2 activity, this might suggest a clinical strategy in PKD arising from mutations in PKD1 (in which the PKD2 gene is structurally

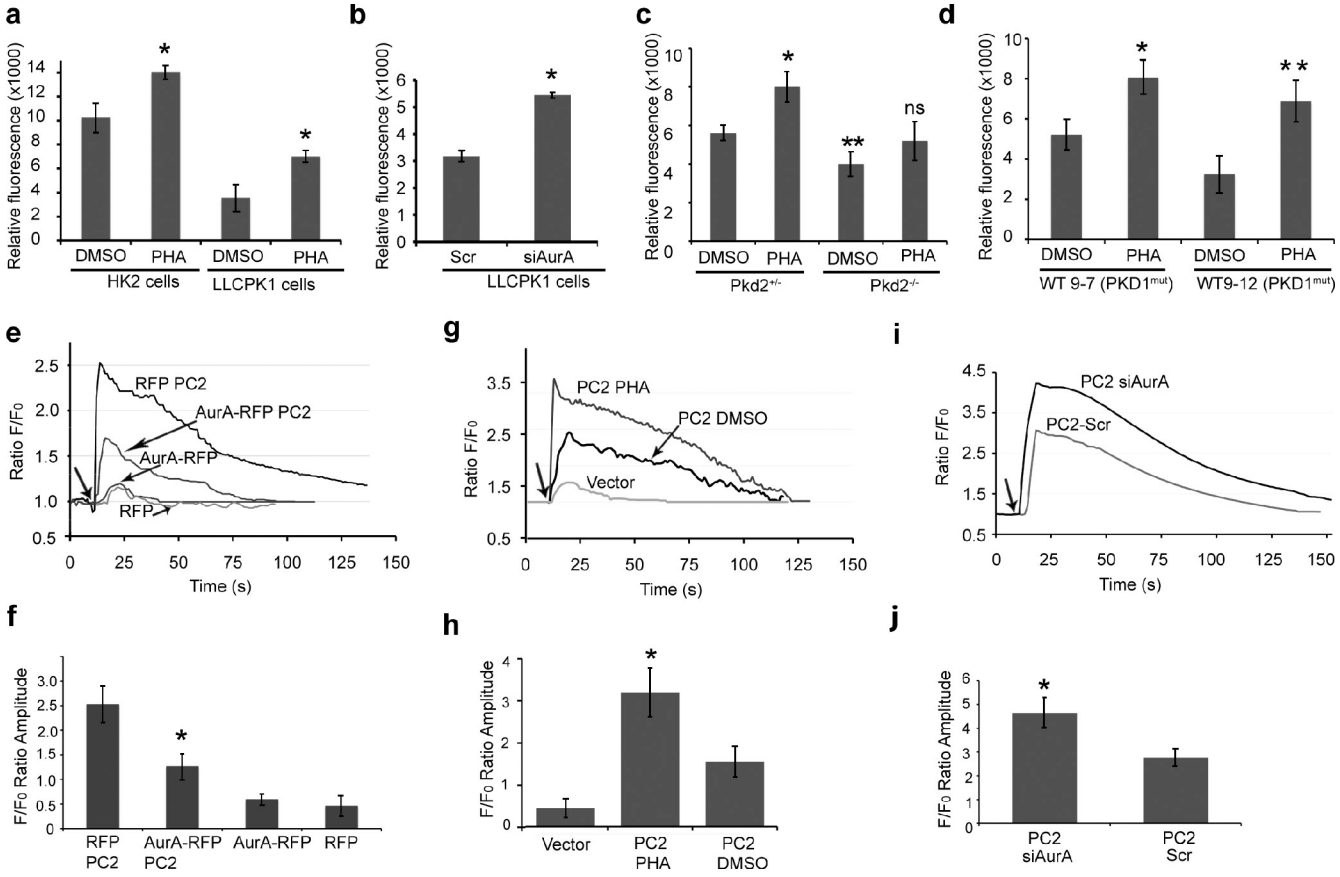

Figure 3. **AurA negatively regulates basal cellular Ca^{2+} levels and PC2-dependent Ca^{2+} channel activity.** (a) Effect of PHA-680632 on basal intracellular Ca^{2+} in HK-2 and LLCPK1 cells. Cells were loaded with 5 µM Fluo-4 AM, which autofluoresces upon binding cytoplasmic Ca^{2+}. Cells were treated with PHA-680632 (PHA) to inhibit Aurora kinase, or DMSO vehicle control. *, P = 0.0024; **, P = 0.0013. (b) Basal Ca^{2+} level in LLCPK1 cells treated with siRNA to deplete AurA (siAurA) versus scrambled siRNA control (Scr). *, P = 0.00056. (c) Basal Ca^{2+} levels were assessed in $Pkd2^{-/-}$ and $Pkd2^{+/-}$ cells treated with PHA-680632 or DMSO. *, P = 0.0132; **, P = 0.0209 (in comparison with DMSO-treated $Pkd2^{+/-}$ cells); and P > 0.05 (NS) in comparison with DMSO-treated $Pkd2^{-/-}$ cells. (d) Basal Ca^{2+} levels were assessed in two PKD1 mutant cell lines, WT9-7 and WT9-12, treated with PHA-680632 or DMSO. *, P = 0.0098; **, P = 0.0107. For a–d, all data are expressed as the means ± SEM from at least three independent experiments (n > 50 in each experiment). (e) HEK293 cells transiently cotransfected 48 h previously with plasmids expressing PC2 and AurA-RFP or control RFP were loaded with 5 µM Fluo-4 AM before analysis. Immunofluorescence was measured before and after addition of AVP (indicated by arrows in e, g, and i). Data are presented as the F/F_0 ratio, indicating increase in signal over unstimulated cells. F, fluorescence intensity; F_0, baseline fluorescence intensity. (f) For this and subsequent experiments, the mean increase in amplitude (±SEM) of AVP-induced cytoplasmic Ca^{2+} transients was calculated from n > 50 RFP-positive cells in each of three experiments. The asterisks shows that, for AurA-RFP, amplitude decreased versus RFP controls; P = 0.008. Alternative analysis as AUC is shown in Fig. S3 a. (g) HEK293 cells transfected 48 h previously with a plasmid expressing PC2 or vector control and pretreated for 2 h with 500 nM PHA-680632 or DMSO vehicle were analyzed as in e. (h) Quantification of data in f. The asterisk indicates that PHA-680632 increased amplitude of signal versus DMSO; P = 0.0007. Analysis as AUC is shown in Fig. S3 b. (i) siRNA depletion of AurA in HK-2 cells increases amplitude of Ca^{2+} release versus scrambled control. (j) Quantification shows significant difference in amplitude (*, P = 0.0055). Analysis as AUC is shown in Fig. S3 c.

intact). In vivo, Aurora kinase inhibitors have marked effects as cell cycle inhibitors (Gautschi et al., 2008), which is relevant to their action in cancer therapy, raising the possibility of toxic side effects if these agents were used in PKD. However, a recent study has suggested that the cytotoxic effects of Aurora kinase inhibitors used in vivo at least partially reflects their cross-reactive inhibition of Aurora B rather than AurA, which occurs at higher concentrations (discussed in Gautschi et al., 2008).

We compared the doses of PHA-680632 required to inhibit cell growth with those required to enhance PC2 signals. In HK-2 cells, the half-maximal IC (IC_{50}) value for PHA-680632 is 3.25 µM, whereas the 500-nM concentration used for the aforementioned experiments represents an IC_5 value (Fig. 4 a). In contrast, an approximately twofold enhancement of AVP-induced Ca^{2+} release is seen whether PHA-680632 is used either at 3.25 µM or at 500 nM (Fig. 4, b and c; and Fig. S3 d). One possible explanation for the difference in results could be that PHA-680632 was used for only a 2-h pretreatment in Ca^{2+} release experiments but must be sustained in culture medium for 3 d in IC_{50} determinations: greater compound decay in the latter experiments might stipulate higher initial dosing concentrations. However, in parallel experiments in which PHA-680632 was added to media 2 or 24 h before AVP treatment, significantly greater enhancement of PC2 activity occurred with the longer 24-h preincubation than the 2-h incubation used for other experiments, suggesting drug stability was not an issue (Fig. 4, b and c). These data suggest that AurA may be a useful target in modulating PC2 activity in vivo.

AurA interacts directly with PC2

The bulk (>95%) of intracellular PC2 associates with the ER and mediates Ca^{2+} release to the cytoplasm (Cai et al., 1999). To assess whether there might be direct interactions between AurA,

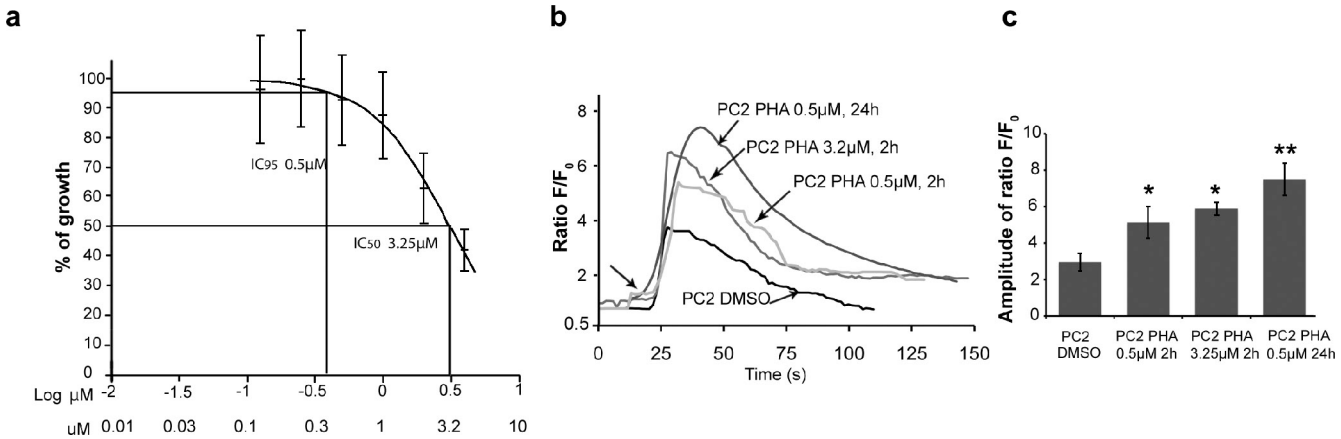

Figure 4. **PHA-680632 enhances PC2 activity at low IC values.** (a) IC_{50} curve for PHA-680632 (PHA) treatment of HK-2 cells stably expressing PC2. Cell viability was detected by Alamar blue assay 72 h after treatment. (b) HK-2 cells stably expressing PC2 were treated with DMSO or with PHA-680632 at concentrations of 0.5 or 3.25 μM for 2 or 24 h before AVP stimulation and determination of the F/F_0 ratio. Addition of AVP is indicated by the first arrow. (c) Quantification of relative F/F_0 amplitude of data in b. Difference between the double asterisks and single asterisks is significant, P = 0.0022; the difference between the single asterisks is not significant. Analysis as AUC is shown in Fig. S3 d. F, fluorescence intensity; F_0, baseline fluorescence intensity. Error bars indicate SEM.

its previously defined partner and activator NEDD9 (Pugacheva and Golemis, 2005), and PC2, we first established that endogenous AurA and PC2 coimmunoprecipitated from HK-2 cells (Fig. 5 a, left) and from primary kidney lysate (Fig. 5 a, middle). Furthermore, the coimmunoprecipitation was clearly observed in lysates prepared from $Pkd2^{+/-}$ cells but not in lysates from $Pkd2^{-/-}$ cells (Fig. 5 a, right). We next cotransfected AurA with the GFP-tagged PC2 cytoplasmic C-terminal domain (PC2-CT, aa 779–968) into HEK293 kidney cells. Overexpressed AurA and PC2-CT coimmunoprecipitated (Fig. 5 b and Fig. S2 a). Furthermore, in a defined in vitro system, recombinant purified full-length AurA pulled down GST-fused PC2-CT (Fig. 5 c and Fig. S2 b), interacting separately with both the AurA regulatory and catalytic domains (Fig. 5 d). The PC2 C terminus contains the primary sites for interaction with PC1 (aa 832–895). AurA did not compete with PC1 for binding to PC2 (Fig. 5 e), suggesting the utilization of distinct binding sites on PC2.

Finally, in contrast to the results with AurA, although overexpressed NEDD9 and PC2 coimmunoprecipitated (Fig. 5 f), no interaction was seen between endogenous NEDD9 and PC2 or the two purified proteins in vitro system (not depicted). However, the presence of NEDD9 enhances the interaction between AurA and PC2, as siRNA depletion of NEDD9 significantly depleted the degree of coimmunoprecipitation between AurA and PC2-CT from HEK293 cells overexpressing these two proteins (Fig. S2 c). Together, these data suggested a strong and direct interaction between AurA and the PC2 C terminus and a significantly weaker or indirect interaction between NEDD9 and PC2 that nevertheless contributed to efficient interactions between AurA and PC2.

AurA phosphorylates PC2 on C-terminal residue S829

Besides the PC1 interaction motif, the PC2 C terminus (Fig. 6 a) encompasses an EF hand, Ca^{2+}-binding motif (aa 754–782), and ER-targeting sequences (aa 787–820; Giamarchi et al., 2006). A S812 CK2 (casein kinase 2) phosphorylation site is important for positively regulating PC2 Ca^{2+} channel activity (Cai et al., 2004). We identified a strongly consensus candidate AurA phosphorylation motif (Ferrari et al., 2005) at residue S829 (RRGSI), adjacent to the ER-targeting domain, and a less favorable motif at residue S944 (PRSSR). We established that recombinant activated AurA phosphorylated the PC2 C terminus in vitro (Fig. 6 b). AurA phosphorylation of PC2 was enhanced by interactions with NEDD9 (Pugacheva and Golemis, 2005) in contrast to AurA phosphorylation of the control substrate MBP, which was unaffected (Fig. 6 c). AurA phosphorylation of PC2 was separately enhanced by inclusion of CaM and Ca^{2+} in in vitro reactions (Fig. 6 d).

We next compared the ability of AurA to phosphorylate a wild-type PC2 C terminus versus derivatives with S→A mutations in the S829, S944, or CK2 motifs or combinations of these mutations (Fig. 6, e and f). An S829A mutation greatly reduced AurA phosphorylation of PC2, resulting in levels close to the background GST negative control, whereas S944A and S812A had no effect on this phosphorylation, either independently or in combination with S829A. By comparison, CK2 phosphorylation was reduced to a comparable degree solely by mutation of the S812 residue, whereas CK2 phosphorylation of PC2 was not affected by the presence of S829A or S944A mutations (Fig. 6, g and h). To investigate the in vivo phosphorylation of the S829 site, we exploited the fact that this site is quite similar to the general PKA substrate consensus (RRxS). Phospho-PKA substrate antibody recognized PC2, but not S829A-mutated PC2, in transiently transfected HEK293 cells (Fig. 6, i and j). Importantly, cotransfection of constitutively active AurA (T288D) increased phosphorylation of this site, whereas treatment of cells with an AurA inhibitor (PHA-680632), but not a PKA inhibitor (H89), reduced in vivo phosphorylation. Similar results were obtained using two additional small molecule inhibitors of AurA and after depletion of either AurA or NEDD9 by siRNA (Fig. S2, d and e). Those data indicate that full-length PC2 is phosphorylated in vivo at S829.

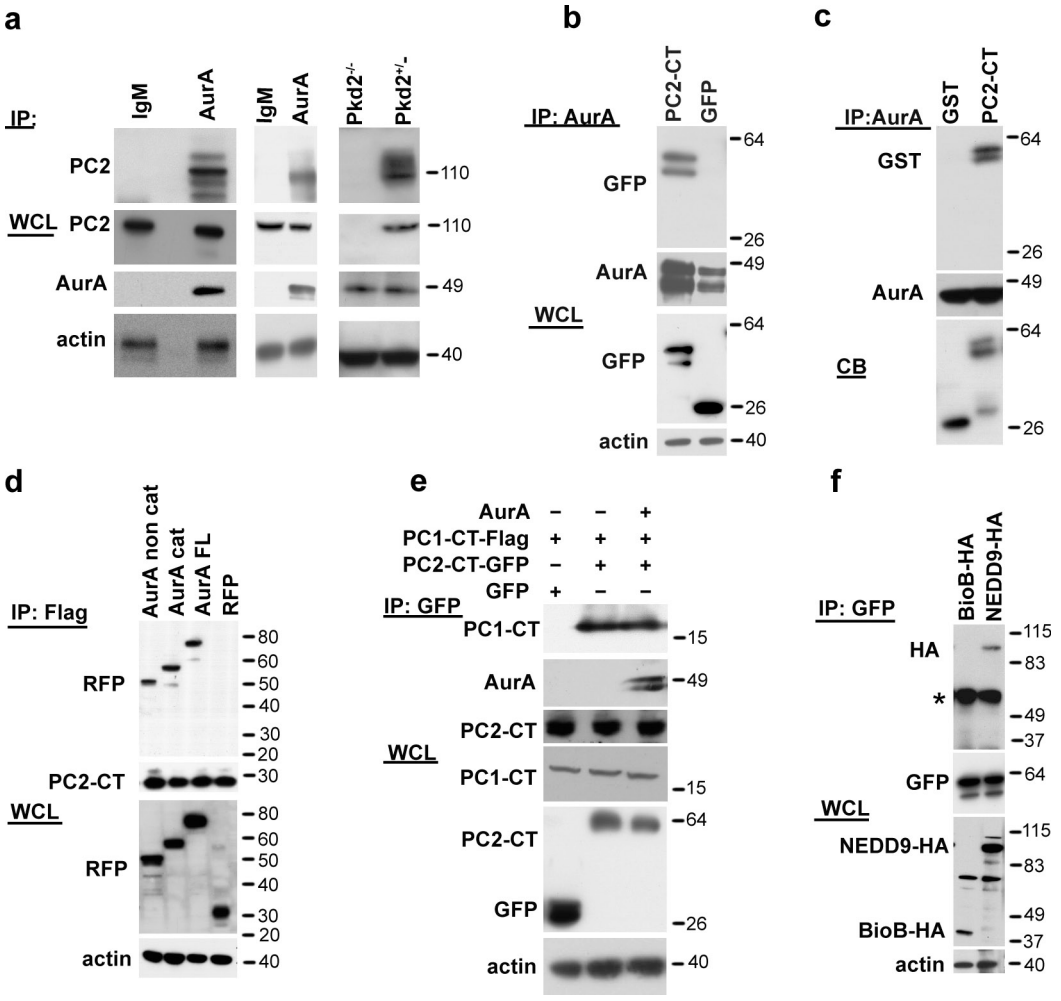

Figure 5. **AurA interacts directly with PC2.** (a) Antibody to AurA or control IgM was used for immunoprecipitation (IP) from HK-2 cells (left), mouse kidney lysates (middle), or PKD2$^{-/-}$ and PKD2$^{+/-}$ cells (right) followed by Western blotting with antibodies to AurA or PC2 (YCC2) as indicated. The strong band migrating at ∼110 kD represents native PC2, with faster migrating bands reflecting degradation products and slower migrating bands showing glycosylated species. (b) Antibody to AurA was used for immunoprecipitation from whole-cell lysates (WCL) transfected with plasmids expressing AurA and either GFP-PC2$_{779–968}$ or GFP followed by Western blotting with the indicated antibodies. Reverse orientation immunoprecipitation is shown in Fig. S2 f. (c) Antibody to AurA was used in immunoprecipitation from the in vitro mixture containing GST-PC2$_{779–968}$ or GST only and recombinant His-AurA. CB indicates Coomassie blue staining of starting material. Reverse orientation pull-down is shown in Fig. S2 g. (d) RFP-fused catalytic (cat; aa 132–403) and noncatalytic (noncat; aa 1–131) domains of AurA or full-length (FL) AurA-RFP coexpressed with Flag-PC2$_{779–968}$ into HEK293 cells and immunoprecipitated with the Flag antibody followed by Western blotting with the indicated antibodies. (e) HEK293 cells were cotransfected with plasmids expressing combinations of GFP, GFP-PC2$_{779–968}$, or Flag-PC1-CT$_{4191–4302}$ and AurA as indicated. Cell lysates were immunoprecipitated using the anti-GFP antibody and visualized with antibodies indicated in the Western blot analysis. (f) Plasmids expressing HA-NEDD9, HA-BioB, and GFP-PC2$_{779–968}$ were transfected into HEK293 cells, cell lysates were immunoprecipitated with the antibody to GFP, and Western blotting was performed with the indicated antibodies. The asterisk indicates immunoglobulin heavy chain. Molecular masses are given in kilodaltons.

We have analyzed the consequences of AurA phosphorylation on PC2 expression, localization, and activity. PC2 is known to localize to the ER membrane, ciliary membrane, and plasma membrane. PC2 localized to the ER and to cis portions of the Golgi apparatus are sensitive to endoglycosidase H cleavage, whereas plasma membrane– and cilia-localized forms of PC2 are not (Cai et al., 1999; Koulen et al., 2002). The AurA inhibitor PHA-680632 did not affect the overall abundance of PC2 or the pool size of endoglycosidase H–cleavable PC2, whether in ciliated or nonciliated HK-2 cells (Fig. S2 f). Subsequent immunofluorescence analysis indicated the degree of localization of the S829A mutant to the ER and cilia is comparable with that of wild-type PC2 (Fig. S2, g and h). However, the mutation of the AurA phosphorylation site significantly affected ER integrity, with the ER of cells expressing these mutants invariably with an abnormal aggregated morphology within 24 h (Fig. S2 h) and dying within 48–72 h of transfection or transduction. This limitation made it impossible to reliably assess the consequence of the S829A mutation on PC2 channel activity against a context of dying cells.

Discussion

The work presented here reveals a completely novel activity of AurA in the control of cellular homeostasis for calcium. We have previously shown that transient stimuli, such as AVP or histamine, trigger Ca^{2+} release to the cytoplasm, inducing CaM binding and autoactivation of AurA, which is marked by AurA

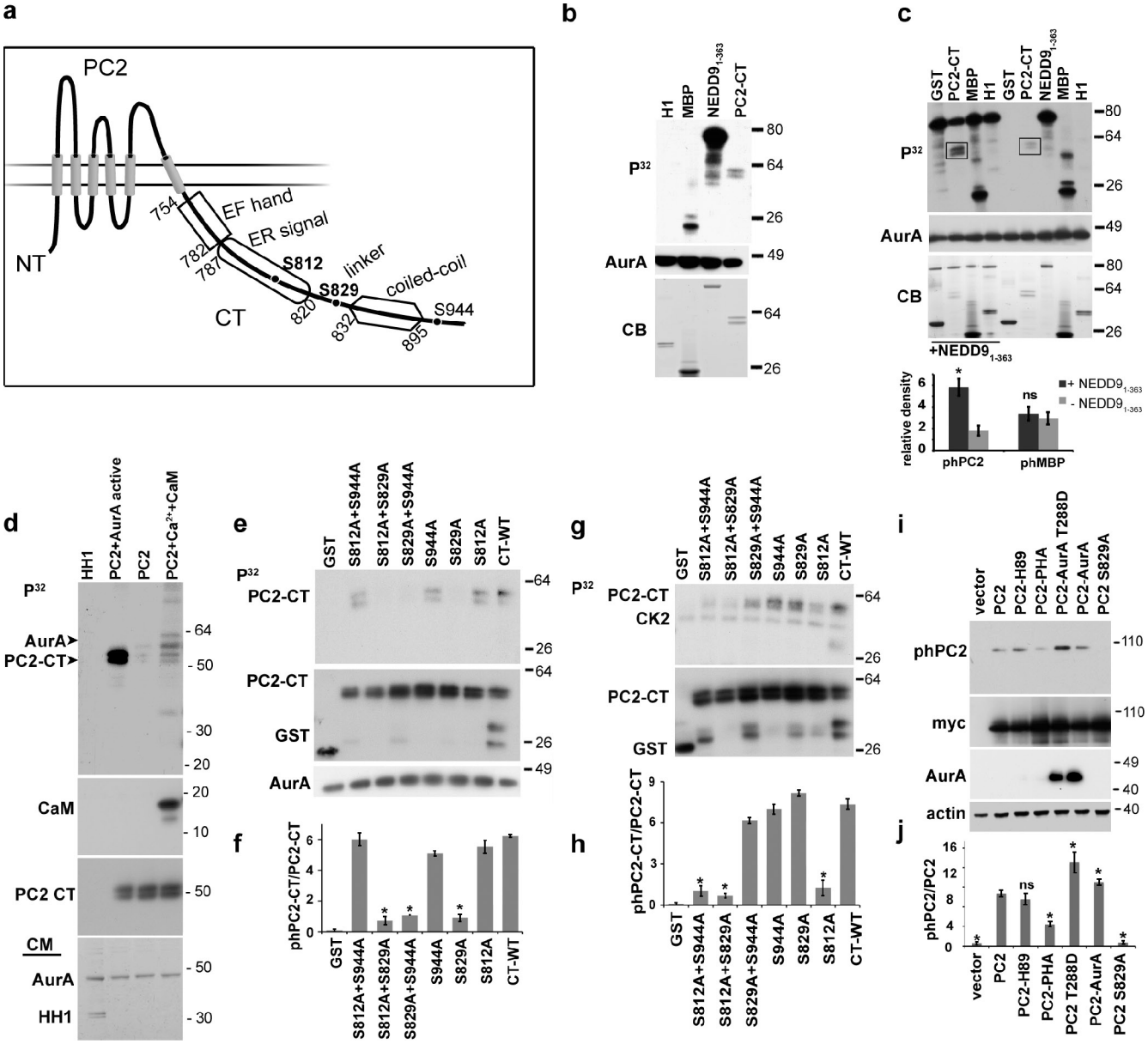

Figure 6. **AurA phosphorylates PC2 on C-terminal residue S829.** (a) Structural motifs on PC2 C-terminal (CT) domain include PC1-binding motif (coiled-coil domain; aa 832–895), an EF hand for Ca^{2+} binding (EF-hand; aa 754–782), and ER-targeting sequences (aa 787–820). Location of assessed sites for CK2 (S812) and AurA (S829 and S944) phosphorylation are indicated. NT, N-terminal. (b) Bacterially expressed GST-$PC2_{779–968}$ or GST-$NEDD9_{1–363}$ and MBP (positive controls) or histone H1 (H1) were incubated with recombinant active AurA kinase in an in vitro kinase assay with γ-[^{32}P]ATP. The reactions were resolved by SDS-PAGE and analyzed by autoradiography, Coomassie blue (CB) staining, and Western blotting with the antibody to AurA. (c) Experiment as in b, except GST-$NEDD9_{1–363}$ was included in the indicated reactions, and relative phosphorylation of PC2 and MBP were calculated (graph). Data are expressed as mean values ± SEM of three experiments. *, $P < 0.001$. For analysis, phosphorylation of PC2 and MPB was first normalized to total PC2 and total MBP and then further normalized to AurA levels. The boxes indicate phosphorylated species of the C-terminal tail of PC2. (d) Bacterially expressed GST-$PC2_{779–968}$ was incubated with recombinant preactivated AurA (AurA active) or AurA purified from baculovirus in an in vitro kinase assay in the presence or absence of PC2, CaM, and Ca^{2+} as indicated. (top) autoradiography; (bottom) Western blots with the indicated antibodies. (e and f) GST-fused derivatives of $PC2_{779–968}$ with mutations affecting a previously defined CK2 site ($PC2_{S812A}$) and two candidate AurA sites ($PC2_{S829A}$ and $PC2_{S944A}$) alone or in combination were used in in vitro kinase reactions with recombinant AurA. Phosphoimaging of autoradiographs from three independent experiments was quantified (f), and the relative phosphorylation of $PC2_{779–968}$ mutants was calculated (graph). Data are expressed as mean values ± SEM of three experiments. *, $P < 0.001$. (g and h) Experiments as in e and f, except recombinant CK2 was used rather than AurA. *, $P < 0.001$. (i) Lysates from HEK293 cells overexpressing Myc-tagged PC2 or the Myc-tagged S829A PC2 mutant (Myc) in the presence or absence of AurA or T288D (catalytically active) AurA were used for immunoprecipitation. Cells were treated with 10 µM H89 PKA inhibitor or 500 nM PHA-680632 (PHA) AurA inhibitor for 3 h as indicated. RRxS-directed antibody was used to visualize phosphorylation of the S829 residue (phPC2). Western blot of coimmunoprecipitation from three independent experiments was quantified (j), and relative phosphorylation of PC2 was calculated. Difference versus PC2: *, $P < 0.05$. WT, wild type.

S^{51} phosphorylation (Plotnikova et al., 2010). We have now found that AurA negatively regulates the basal Ca^{2+} level of renal cells and PC2-dependent Ca^{2+} release. We have also shown that AurA binds and phosphorylates PC2 at S^{829}, with AurA phosphorylation of PC2 observed both in defined in vitro reactions and in cells. NEDD9 contributes to the specific interaction of

AurA with PC2, likely by promoting the ability of AurA to phosphorylate PC2. Inhibition of AurA by small molecule inhibitors enhances PC2 activity, increasing the magnitude of ER Ca^{2+} release induced by upstream activators. Our findings that AurA is abundant and frequently active in normal kidney tissue and abnormally expressed in PKD-associated renal cysts together provide strong evidence that changes in AurA function may be relevant to the pathogenesis of PKD.

Interestingly, studies of AurA in cancer have often suggested the pro-oncogenic activity of AurA may arise because its overexpression allows a normally centrosomal protein access to inappropriate substrates. However, our results suggest changes in AurA expression in cancer may promote quantitative changes in AurA activity more than qualitative phosphorylation of novel substrates. As based on the data presented here, AurA has a broader subcellular localization profile in untransformed kidney cells than is commonly appreciated, with the centrosome acting as a concentration point at which the protein is most readily visualized. This broader view of AurA activity is compatible with recent reports that AurA phosphorylates proteins, such as RalA (Wu et al., 2005), which are not known for centrosomal localization (Clough et al., 2002). Our data indicate that not only kidney cells but also primary kidney tissue expresses significant quantities of AurA in the cytoplasm and nucleus. They further show that some of this AurA is activated in noncycling cells in normal kidney tissue, particularly in cells of the distal convoluted tubules that collect ducts from which cysts arise. AurA expression and activation are further elevated and anomalous in cysts. In this context, it is interesting that two recent studies linked AurA to the function of VHL, one showing direct binding between the two proteins (Ferchichi et al., 2010), and a second showing that mutation of VHL in renal cell carcinoma induces both AurA and its partner Nedd9/HEF1 (Xu et al., 2010). Loss of VHL is a major lesion responsible for the development of renal cell carcinoma, which frequently has associated cysts.

In general, calcium signaling differs significantly in cancerous (Roderick and Cook, 2008) and cystic (Harris and Torres, 2009) cells versus normal cells, promoting increased cell proliferation through the abnormal activation of numerous calcium-responsive signaling pathways. The fact that AurA activation was elevated in PKD-associated cysts is interesting and may reflect paradoxical activation in the context of mutated PKD1 and PKD2, analogous to the overexpression of growth inhibitory proteins in tumors that have eliminated partners in a feedback loop. The specific mechanism of AurA activation in this pathological condition bears further investigation. However, based on our results, inappropriately activated AurA may act as an intermediate in some of signaling processes relevant to PKD. For example, besides binding the PC2 partner Id2, NEDD9 directly binds and is both a target and activator of Src kinase (recently discussed in Singh et al., 2007). Src signaling is abnormal in PKD, and a recent study has indicated that inhibition of Src produces clinical benefits in PKD (Sweeney et al., 2008). Through interactions with NEDD9, AurA may influence the activity of Src and Id2 in either normal renal tissue or in cysts. These close physical interactions suggest further topics of study not only in renal cysts but also in cancer, in which NEDD9, Src, and Id2 all have oncogenic functions. We note that the fact that the activity of AurA inhibitors was reduced, but not completely eliminated, in $Pkd2^{-/-}$ cells suggests that PC2 is an important mediator of AurA action in calcium signaling but perhaps not the only relevant AurA target; proteins such as the ryanodine receptor and inositol-1,4,5-triphosphate receptor are also mediators of release of calcium from the ER (Anyatonwu and Ehrlich, 2004) and may be influenced by AurA.

Previous studies have identified several regulatory phosphorylation sites on PC2. These include phosphorylation by GSK3 (glycogen synthase kinase 3) at S^{76}, CK2 at S^{812}, and protein kinase D at S^{801} (Cai et al., 2004; Streets et al., 2006, 2010). These phosphorylation events affect the localization and Ca^{2+} channel activity of PC2, its interaction with partners, such as Id2, and the ability of PC2 to support cell growth (Cai et al., 2004; Köttgen et al., 2005; Li et al., 2005; Streets et al., 2006, 2010). The phosphorylation at S^{801} within the ER-targeting domain is essential for Ca^{2+} release from the ER (Streets et al., 2010). In contrast, the highly toxic effect of overexpressing the S829A derivative of PC2 in cells, which is accompanied by a "collapsed" morphology to the ER itself, suggests, as one possibility, that this residue may cause gross structural changes in PC2 that damage ER structural integrity while not affecting targeting to the ER.

There is a potential therapeutic benefit to identifying ways to stimulate PC2 channel activity, and there is an urgent need to develop effective therapies for PKD. At present, several targeted therapeutic agents are moving through preclinical development and clinical trials. Besides c-Src, these include agents targeting mammalian target of rapamycin, HER2, and others. These studies provide a precedent for adapting drugs originally developed as cancer therapeutics in PKD. An obvious concern is that, given the chronic but survivable nature of PKD, it is necessary to be extremely cautious in using powerful compounds that may themselves ultimately select for oncogenic changes. However, our data suggest that very low doses of an AurA-targeting inhibitor are able to enhance PC2 activity, suggesting a basis for further investigation of such agents in cases of PKD linked to the *PKD1* mutation, in which PC2 is insufficiently activated but structurally intact. It is also fascinating to note that defects in *PKD1* and *PKD2* have recently been linked to centrosomal amplification in both animal models and human patients (Battini et al., 2008; Burtey et al., 2008), reducing the separation between cystic syndromes and cancer and, perhaps, supporting the idea that calcium-dependent activation of AurA is relevant to the severity of PKD presentation. Encouragingly, a calcimimetic drug was recently shown to have promise in inhibiting cystic growth in PKD (Gattone et al., 2009). There is clearly much room for further investigation.

Materials and methods

Plasmids and constructs

Lentiviral constructs were obtained by cloning full-length *PKD2* into the pLV-CMV-H4-puro vector (provided by P. Chumakov, Russian Academy of Sciences, Moscow, Russia, and A. Ivanov, West Virginia University, Morgantown, WV). *PKD2* cloned in pcDNA3.1-Myc was provided by S. Somlo (Yale University, New Haven, CT). The *PKD2*-CT fragment (aa 779–968) was cloned into the pEGFP (Takara Bio Inc.) and pGEX-6P1 vectors (Millipore). Amino acid substitution mutations were introduced into wild-type human *PKD2* cDNA by site-directed mutagenesis using a

site-directed mutagenesis kit (QuikChange XL; Agilent Technologies). The Flag-fused C-terminal domain of PKD1 (aa 4,191–4,302) containing the PC1–PC2 interaction site was cloned in the pcDNA3.1(+) vector (Invitrogen). Flag- and GST-fused NEDD9 were expressed from the vectors pCatch-Flag (O'Neill and Golemis, 2001) and pGEX-2T (Law et al., 1998), respectively. AurA and derivatives were expressed from pCMV-SPORT6-C6 (Thermo Fisher Scientific) and pcDNA3.1–monomeric RFP vectors. A PCR product of monomeric RFP1 was ligated into pcDNA3.1(+) (Invitrogen) to create pcDNA3.1–monomeric RFP. pLV-CMV-H4-puro vector, pEFGP, pcDNA3, and HA-BioB (an extensively truncated *Escherichia coli* BioB expressed from pcDNA3.1-6HA) were used for negative controls (Singh et al., 2008).

Cell culture and transfection

HEK293 cells were maintained in DME with 10% FBS plus penicillin/streptomycin. LLCPK1 (CRL-1392; American Type Culture Collection) cells were maintained in DME/F12 (1:1) with 5% of FBS. The immortalized human kidney proximal tubular cell line (HK-2; catalog no. CRL-219; American Type Culture Collection) was grown to subconfluence in keratinocyte media (Invitrogen). $Pkd2^{-/-}$ and $Pkd^{+/-}$ were provided by S. Somlo and have been previously described (Grimm et al., 2003). PKD1 mutation–containing WT9-7 (CRL-2830; American Type Culture Collection) and WT9-12 (CRL-2833; American Type Culture Collection) immortalized epithelial cells from ADPKD kidney cysts (Loghman-Adham et al., 2003) were grown in DME with 10% of FBS on flasks coated with 3 mg/ml bovine collagen type I solution. We transiently transfected HEK293 cells with expression constructs for *PKDCT*, *PKD2*, *NEDD9*, and *AurA* using Lipofectamine and Plus reagent (Invitrogen) according to the manufacturer's instructions. Cells were used for electrophysiological experiments 24–48 h after transfection. For lentiviral infection, pLV constructs were cotransfected with pVSV-G and psPAX2 into the packaging cell line 293-T. After 24 h, media were collected, filtered through a 0.45-µm polyvinylidene fluoride filter (Millipore), and applied to HK-2 cells with 8 µg/µl polybrene (Sigma-Aldrich) for 2 d, with fresh viral supernatant added every 12 h. After 48 h, cells were lysed, analyzed by Western blot analysis, and used for further experiments. HK-2 cells stably expressing PC2 were obtained by infecting the HK-2 cell line with the pLV-*PKD2* lentiviral vector and then selecting for 6–10 d with 1 mg/ml puromycin to produce a mass culture as in Pugacheva and Golemis (2005). PC2 expression was verified by immunoblot and immunofluorescence analyses. Transient transfection of siRNAs was performed using transfection reagent (RNAiMAX; Invitrogen). Cells were assayed after 48 h of transfection. RNA oligonucleotide duplexes targeted to NEDD9 (Hs_NEDD9_2 [SI00657370], 5′-CGCTGCCGAAATGAAGTATAA-3′, and Hs_NEDD9_1 [SI00657363]) and AurA (Hs_STK6_5 [SI03114111] and Hs_AURKA_1_HP [SI00053452], 5′-TCCCAGCGCATTCCTTTGCAA-3′) were purchased from QIAGEN as well as scrambled negative controls. After transfection of siRNAs, the degree of depletion of target proteins was determined by Western blotting. IC_{50} determinations with the AurA kinase inhibitor PHA-680632 (Nerviano Medical Sciences) were performed as in Skobeleva et al. (2007).

Immunofluorescence

Cells grown on coverslips were fixed with 4% paraformaldehyde for 10 min and then cold methanol for 5 min, permeabilized with 1% Triton X-100 in PBS, blocked in PBS with 3% BSA, and incubated with antibodies using standard protocols. Primary antibodies included mouse anti-AurA (BD), anti-acetylated α-tubulin mAb (clone 6-11B-1 [Sigma-Aldrich] and clone K(Ac)40 [Enzo Life Sciences]), anti-PC2 (G20 [Santa Cruz Biotechnology, Inc.] and YCC2 [a gift from S. Somlo]), and mouse anti–protein disulfide isomerase mAb (Abcam). Secondary antibodies labeled with Alexa Fluor 488, Alexa Fluor 568, and DAPI to stain DNA were obtained from Invitrogen. Confocal microscopy was performed using a confocal microscope (C1 Spectral; Nikon) equipped with an NA 1.40 oil immersion 60× Plan Apochromat objective (Nikon). Images were acquired at RT using EZ-C1 3.8 (Nikon) software and analyzed using the imaging MetaMorph (Molecular Devices) and Photoshop (version CS2; Adobe) software. Adjustments to brightness and contrast were minimal and were applied to the whole image.

Protein expression, Western blotting, and immunoprecipitation

Recombinant GST, GST fused to aa 779–968 of the PC2 C terminus (GST-$PC2_{779–968}$), and NEDD9 (aa 1–363; previously shown to bind and activate AurA; Pugacheva and Golemis, 2005) were expressed in BL21 (DE3) bacteria, induced with IPTG, and purified using a purification module (MicroSpin GST; GE Healthcare). Purified recombinant AurA was purchased from Millipore. For Western blotting and immunoprecipitation, mammalian cells were disrupted in lysis buffer (CelLytic M; Sigma-Aldrich) supplemented with a protease and phosphate inhibitor cocktails (Roche). Whole-cell lysates were used either directly for SDS-PAGE or for immunoprecipitation. Immunoprecipitation samples were incubated overnight with an antibody at 4°C and subsequently incubated for 2 h with protein A/G–Sepharose (Thermo Fisher Scientific), washed, and resolved by SDS-PAGE. GST pull-down assays used wild-type AurA (Millipore) mixed with titrated quantities of GST and GST-$PC2_{779–968}$.

Western blotting was performed using standard procedures and developed by chemoluminescence using the West Pico system (Thermo Fisher Scientific). Primary antibodies included mouse anti-AurA (BD), anti-phAurA-T^{288} (Cell Signaling Technology), anti-Myc (Santa Cruz Biotechnology, Inc.), anti–β-actin mAb (AC15; Sigma-Aldrich), and anti-PC2 (G20 [Santa Cruz Biotechnology, Inc.] and YCC2 [a gift from S. Somlo]). Rabbit anti-GFP (ab290; Abcam) was used for immunoprecipitation, and mouse anti-GFP (JL-8; BD) was used for Western blotting. Anti-GST mAb (Cell Signaling Technology), polyclonal red anti-Flag M2 affinity gel (EZview; Sigma-Aldrich), and polyclonal anti-AurA agarose immobilized conjugate (IgM; Bethyl) were used for immunoprecipitations. Secondary anti–mouse and anti–rabbit HRP-conjugated antibodies (GE Healthcare) were used at a dilution of 1:10,000 for visualization of Western blots. Image analysis was performed using ImageJ image processing and analysis software (National Institutes of Health) with the signal intensity normalized to β-actin or total AurA level.

To assess the AurA phosphorylation of PC2 in vivo, Myc-tagged PC2 was transiently expressed alone or with AurA or T288D-AurA in HEK293 cells and then immunoprecipitated with the anti-Myc antibody. Phosphorylation of the S^{829} site was assessed by Western blotting with Phospho-(Ser/Thr) PKA Substrate Antibody (Cell Signaling Technology). 500 nM PHA-680632, 4 µM C1368 (Sigma-Aldrich), or 50 nM MLN8237 (Millennium Pharmaceuticals, Inc.) was used to inhibit AurA, and 10 µM H89 PKA inhibitor (EMD) was used to inhibit phosphorylation. For analysis of PC2 glycosylation, cell lysates were treated with endoglycosidase H (New England Biolabs, Inc.) and analyzed by SDS-PAGE followed by immunoblotting as previously described (Cai et al., 1999; Koulen et al., 2002).

Kinase assays

To assess phosphorylation of PC2 by AurA, an in vitro kinase assay was performed using bacterially expressed GST-fused PC2-CT and recombinant active AurA or overexpressed AurA immunoprecipitated from mammalian cells in standard kinase buffer with the addition of an Mg/ATP cocktail (Millipore). MBP (Millipore) and histone H1 (Millipore) were used as positive and negative controls for AurA phosphorylation using standard methods. Parallel aliquots without γ-[^{32}P]ATP were processed for SDS-PAGE/Coomassie staining (Invitrogen). To assess CaM-dependent AurA activation, an in vitro kinase assay was performed using AurA purified from baculovirus or according the protocol described in the previous sentence in the presence of 1 µM CaM (EMD) and 1 mM Ca^{2+}.

Cytosolic Ca^{2+} measurements

Cells expressing PC2 constructs were plated on glass coverslips and grown to ∼80% subconfluence. The coverslips were rinsed in HBSS and incubated with 5 µM Fluo-4 AM in HBSS (Invitrogen) in the presence of 0.02% pluronic acid (Invitrogen) and 2.5 mM probenecid (Invitrogen) for 20–30 min at RT. The coverslips were washed twice in HBSS, mounted in a perfusion chamber (FC2; Bioptechs), and analyzed with a microscope (C1 Spectral confocal) equipped with an NA 1.40 oil immersion 60× Plan Apochromat objective (Nikon) or an NA 1.3 oil immersion 40× Plan Fluo objective (Nikon). Images were acquired using EZ-C1 3.8 software at RT in HBSS media. Cytosolic Ca^{2+} measurements performed in the absence of extracellular Ca^{2+} were performed on cells washed and assayed in the aforementioned HBSS except that $CaCl_2$ was omitted and 0.5 M EGTA was added. In experiments involving AurA inhibition, cells were treated for 2–3 h with 500 nM PHA-680632 before calcium measurement. Fluo-4 was excited at 488 nm, and emission was time-lapse recorded at 522 nm. Cells were individually selected, and their fluorescence intensities were normalized to baseline and analyzed with MetaMorph and MetaFluor softwares (Molecular Devices). The area under curve (AUC) was measured using a standard macro in Excel (Microsoft). For basal intracellular calcium measurements, we used the same approach described at the beginning of this paragraph.

To compare cellular responses, we examined differences in intensity over time using a generalized linear model assuming γ distribution and log link. We fit the models by generalized estimating of equations assuming an autoregressive correlation structure to account for correlation of observations over time. We included baseline intensity, group, time, and the time–group interaction in the models. To allow for flexible effects over time, we

entered time and the related interactions in the model using restricted cubic splines assuming 5 knots (Harrell, 2001). We used Wald tests to assess p-values of group effects at each time point.

Immunohistochemistry

All tissue samples examined were institutional review board–consented, 10–20-mm sections of formalin-fixed, paraffin-embedded tissues, representing either normal human kidney tissue or kidney tissue from patients diagnosed with ADPKD, and archived at the National Disease Resource Interchange. Information about PKD1 versus PKD2 mutational status is unavailable, but based on disease prevalence, the majority of cases likely reflect mutations in PKD1. Samples analyzed were obtained from eight independent patients based on the analysis of a single formalin-fixed, paraffin-embedded tissue specimen for each patient. A standard two-stage indirect immunoperoxidase staining protocol was used for all tissues (Histostain-Plus kit; Invitrogen), with antigen retrieval buffer obtained from BD. As controls, sections were stained with diluent alone (5% goat serum in Tris-buffered saline), and the antibody was preabsorbed with the immunizing peptide. Incubations with tissue sections were performed at RT for 1 h or at 4°C overnight, and subsequent steps were performed at RT. Sections were counterstained with hematoxylin (Sigma-Aldrich). Antibody to total AurA (anti-BTAK antibody; provided by T. Gritsko, University of South Florida, Tampa, FL; with blocking peptide) was used at a dilution of 1:500, and antibody to phospho-T^{288} AurA was used at 1:100 (Bethyl). Images were acquired at 10 and 40× using a microscope (Eclipse E600; Nikon).

Statistical analysis

Statistical comparisons were made using a two-tailed Student's *t* test. Experimental values were reported as the means ± SEM. Differences in mean values were considered significant at $P < 0.05$. All calculations of statistical significance were made using the InStat software package (GraphPad Software).

Online supplemental material

Fig. S1 shows controls for AurA antibody inhibition and siRNA specificity. Fig. S2 analyzes AurA–NEDD9–PC2 interactions, PC2 localization, and expression of PC2 mutants. Fig. S3 shows the analysis of AUC for Fig. 3 (e–j) and Fig. 4 (b and c). Online supplemental material is available at http://www.jcb.org/cgi/content/full/jcb.201012061/DC1.

We are very grateful to Dr. Brian Egleston for help with the statistical analysis in this study, to Michal Jarnik for help with the cell-imaging analysis, and to Dr. Andres Klein-Szanto for discussion of pathological specimens. We thank the National Disease Research Interchange for PKD tissue samples. We are grateful to Stefan Somlo for the gift of the full-length C-myc-*PKD2* cDNA, for YCC2 antibodies to PC2, and for $Pkd2^{-/-}$ and $Pkd2^{+/-}$ cells. We thank Peter Chumakov and Alexey Ivanov for the pLV-CMV-H4 vector and T. Gritsko for the antibody to AurA. We thank Elena Pugacheva for helpful discussions.

The authors were supported by grants R01 CA63366 and R01 CA113342 from the National Institutes of Health, Tobacco Settlement funding from the State of Pennsylvania (to E.A. Golemis), Ovarian Specialized Program of Research Excellence grant P50 CA083638 (Project 4), by the National Cancer Institute core grant CA06927, and support from the Pew Charitable Fund (to Fox Chase Cancer Center). Additional funds were provided for this project by Fox Chase Cancer Center via institutional support of the Kidney Cancer Keystone Program.

Submitted: 9 December 2010
Accepted: 12 May 2011

References

Anand, S., S. Penrhyn-Lowe, and A.R. Venkitaraman. 2003. AURORA-A amplification overrides the mitotic spindle assembly checkpoint, inducing resistance to Taxol. *Cancer Cell*. 3:51–62. doi:10.1016/S1535-6108(02)00235-0

Anyatonwu, G.I., and B.E. Ehrlich. 2004. Calcium signaling and polycystin-2. *Biochem. Biophys. Res. Commun.* 322:1364–1373. doi:10.1016/j.bbrc.2004.08.043

Bacallao, R.L., and H. McNeill. 2009. Cystic kidney diseases and planar cell polarity signaling. *Clin. Genet.* 75:107–117. doi:10.1111/j.1399-0004.2008.01148.x

Battini, L., S. Macip, E. Fedorova, S. Dikman, S. Somlo, C. Montagna, and G.L. Gusella. 2008. Loss of polycystin-1 causes centrosome amplification and genomic instability. *Hum. Mol. Genet.* 17:2819–2833. doi:10.1093/hmg/ddn180

Bayliss, R., T. Sardon, I. Vernos, and E. Conti. 2003. Structural basis of Aurora-A activation by TPX2 at the mitotic spindle. *Mol. Cell*. 12:851–862. doi:10.1016/S1097-2765(03)00392-7

Benzing, T., and G. Walz. 2006. Cilium-generated signaling: a cellular GPS? *Curr. Opin. Nephrol. Hypertens.* 15:245–249. doi:10.1097/01.mnh.0000222690.53970.ca

Bischoff, J.R., L. Anderson, Y. Zhu, K. Mossie, L. Ng, B. Souza, B. Schryver, P. Flanagan, F. Clairvoyant, C. Ginther, et al. 1998. A homologue of *Drosophila* aurora kinase is oncogenic and amplified in human colorectal cancers. *EMBO J.* 17:3052–3065. doi:10.1093/emboj/17.11.3052

Burtey, S., M. Riera, E. Ribe, P. Pennenkamp, R. Rance, J. Luciani, B. Dworniczak, M.G. Mattei, and M. Fontés. 2008. Centrosome overduplication and mitotic instability in PKD2 transgenic lines. *Cell Biol. Int.* 32:1193–1198. doi:10.1016/j.cellbi.2008.07.021

Cai, Y., Y. Maeda, A. Cedzich, V.E. Torres, G. Wu, T. Hayashi, T. Mochizuki, J.H. Park, R. Witzgall, and S. Somlo. 1999. Identification and characterization of polycystin-2, the PKD2 gene product. *J. Biol. Chem.* 274:28557–28565. doi:10.1074/jbc.274.40.28557

Cai, Y., G. Anyatonwu, D. Okuhara, K.B. Lee, Z. Yu, T. Onoe, C.L. Mei, Q. Qian, L. Geng, R. Wiztgall, et al. 2004. Calcium dependence of polycystin-2 channel activity is modulated by phosphorylation at Ser812. *J. Biol. Chem.* 279:19987–19995. doi:10.1074/jbc.M312031200

Clough, R.R., R.S. Sidhu, and R.P. Bhullar. 2002. Calmodulin binds RalA and RalB and is required for the thrombin-induced activation of Ral in human platelets. *J. Biol. Chem.* 277:28972–28980. doi:10.1074/jbc.M201504200

Ferchichi, I., N. Stambouli, R. Marrackchi, Y. Arlot, C. Prigent, A. Fadiel, K. Odunsi, A. Ben Ammar Elgaaied, and A. Hamza. 2010. Experimental and computational studies indicate specific binding of pVHL protein to Aurora-A kinase. *J. Phys. Chem. B*. 114:1486–1497. doi:10.1021/jp909869g

Ferrari, S., O. Marin, M.A. Pagano, F. Meggio, D. Hess, M. El-Shemerly, A. Krystyniak, and L.A. Pinna. 2005. Aurora-A site specificity: a study with synthetic peptide substrates. *Biochem. J.* 390:293–302. doi:10.1042/BJ20050343

Fischer, E., E. Legue, A. Doyen, F. Nato, J.F. Nicolas, V. Torres, M. Yaniv, and M. Pontoglio. 2006. Defective planar cell polarity in polycystic kidney disease. *Nat. Genet.* 38:21–23. doi:10.1038/ng1701

Foggensteiner, L., A.P. Bevan, R. Thomas, N. Coleman, C. Boulter, J. Bradley, O. Ibraghimov-Beskrovnaya, K. Klinger, and R. Sandford. 2000. Cellular and subcellular distribution of polycystin-2, the protein product of the PKD2 gene. *J. Am. Soc. Nephrol.* 11:814–827.

Gattone, V.H. II, N.X. Chen, R.M. Sinders, M.F. Seifert, D. Duan, D. Martin, C. Henley, and S.M. Moe. 2009. Calcimimetic inhibits late-stage cyst growth in ADPKD. *J. Am. Soc. Nephrol.* 20:1527–1532. doi:10.1681/ASN.2008090927

Gautschi, O., J. Heighway, P.C. Mack, P.R. Purnell, P.N. Lara Jr., and D.R. Gandara. 2008. Aurora kinases as anticancer drug targets. *Clin. Cancer Res.* 14:1639–1648. doi:10.1158/1078-0432.CCR-07-2179

Geng, L., C.R. Burrow, H.P. Li, and P.D. Wilson. 2000. Modification of the composition of polycystin-1 multiprotein complexes by calcium and tyrosine phosphorylation. *Biochim. Biophys. Acta*. 1535:21–35.

Geng, L., W. Boehmerle, Y. Maeda, D.Y. Okuhara, X. Tian, Z. Yu, C.U. Choe, G.I. Anyatonwu, B.E. Ehrlich, and S. Somlo. 2008. Syntaxin 5 regulates the endoplasmic reticulum channel-release properties of polycystin-2. *Proc. Natl. Acad. Sci. USA*. 105:15920–15925. doi:10.1073/pnas.0805062105

Giamarchi, A., F. Padilla, B. Coste, M. Raoux, M. Crest, E. Honoré, and P. Delmas. 2006. The versatile nature of the calcium-permeable cation channel TRPP2. *EMBO Rep.* 7:787–793. doi:10.1038/sj.embor.7400745

Goepfert, T.M., Y.E. Adigun, L. Zhong, J. Gay, D. Medina, and W.R. Brinkley. 2002. Centrosome amplification and overexpression of aurora A are early events in rat mammary carcinogenesis. *Cancer Res.* 62:4115–4122.

Grimm, D.H., Y. Cai, V. Chauvet, V. Rajendran, R. Zeltner, L. Geng, E.D. Avner, W. Sweeney, S. Somlo, and M.J. Caplan. 2003. Polycystin-1 distribution is modulated by polycystin-2 expression in mammalian cells. *J. Biol. Chem.* 278:36786–36793. doi:10.1074/jbc.M306536200

Hanaoka, K., F. Qian, A. Boletta, A.K. Bhunia, K. Piontek, L. Tsiokas, V.P. Sukhatme, W.B. Guggino, and G.G. Germino. 2000. Co-assembly of polycystin-1 and -2 produces unique cation-permeable currents. *Nature*. 408:990–994. doi:10.1038/35050128

Harrell, F.E., Jr. 2001. Chapter 2. *In* Regression Modeling Strategies: with applications to linear models, logistic regression, and survival analysis. F.E. Harrell Jr., editor. Springer, New York. 11–40.

Harris, P.C., and V.E. Torres. 2009. Polycystic kidney disease. *Annu. Rev. Med.* 60:321–337. doi:10.1146/annurev.med.60.101707.125712

Hutterer, A., D. Berdnik, F. Wirtz-Peitz, M. Zigman, A. Schleiffer, and J.A. Knoblich. 2006. Mitotic activation of the kinase Aurora-A requires its binding partner Bora. *Dev. Cell*. 11:147–157. doi:10.1016/j.devcel.2006.06.002

Köttgen, M., T. Benzing, T. Simmen, R. Tauber, B. Buchholz, S. Feliciangeli, T.B. Huber, B. Schermer, A. Kramer-Zucker, K. Höpker, et al. 2005. Trafficking of TRPP2 by PACS proteins represents a novel mechanism of ion channel regulation. *EMBO J.* 24:705–716. doi:10.1038/sj.emboj.7600566

Koulen, P., Y. Cai, L. Geng, Y. Maeda, S. Nishimura, R. Witzgall, B.E. Ehrlich, and S. Somlo. 2002. Polycystin-2 is an intracellular calcium release channel. *Nat. Cell Biol.* 4:191–197. doi:10.1038/ncb754

Kurahashi, T., H. Miyake, I. Hara, and M. Fujisawa. 2007. Significance of Aurora-A expression in renal cell carcinoma. *Urol. Oncol.* 25:128–133. doi:10.1016/j.urolonc.2006.06.001

Law, S.F., J. Estojak, B. Wang, T. Mysliwiec, G.D. Kruh, and E.A. Golemis. 1996. Human enhancer of filamentation 1, a novel p130cas-like docking protein, associates with focal adhesion kinase and induces pseudohyphal growth in *Saccharomyces cerevisiae*. *Mol. Cell. Biol.* 16:3327–3337.

Law, S.F., Y.-Z. Zhang, A.J. Klein-Szanto, and E.A. Golemis. 1998. Cell cycle-regulated processing of HEF1 to multiple protein forms differentially targeted to multiple subcellular compartments. *Mol. Cell. Biol.* 18: 3540–3551.

Law, S.F., Y.-Z. Zhang, S.J. Fashena, G. Toby, J. Estojak, and E.A. Golemis. 1999. Dimerization of the docking/adaptor protein HEF1 via a carboxy-terminal helix-loop-helix domain. *Exp. Cell Res.* 252:224–235. doi:10 .1006/excr.1999.4609

Li, X., Y. Luo, P.G. Starremans, C.A. McNamara, Y. Pei, and J. Zhou. 2005. Polycystin-1 and polycystin-2 regulate the cell cycle through the helix-loop-helix inhibitor Id2. *Nat. Cell Biol.* 7:1202–1212.

Loghman-Adham, M., S.M. Nauli, C.E. Soto, B. Kariuki, and J. Zhou. 2003. Immortalized epithelial cells from human autosomal dominant polycystic kidney cysts. *Am. J. Physiol. Renal Physiol.* 285:F397–F412.

Marumoto, T., D. Zhang, and H. Saya. 2005. Aurora-A - a guardian of poles. *Nat. Rev. Cancer*. 5:42–50. doi:10.1038/nrc1526

Meraldi, P., R. Honda, and E.A. Nigg. 2002. Aurora-A overexpression reveals tetraploidization as a major route to centrosome amplification in p53−/− cells. *EMBO J.* 21:483–492. doi:10.1093/emboj/21.4.483

Mori, D., M. Yamada, Y. Mimori-Kiyosue, Y. Shirai, A. Suzuki, S. Ohno, H. Saya, A. Wynshaw-Boris, and S. Hirotsune. 2009. An essential role of the aPKC-Aurora A-NDEL1 pathway in neurite elongation by modulation of microtubule dynamics. *Nat. Cell Biol.* 11:1057–1068. doi:10.1038/ncb1919

Nauli, S.M., F.J. Alenghat, Y. Luo, E. Williams, P. Vassilev, X. Li, A.E. Elia, W. Lu, E.M. Brown, S.J. Quinn, et al. 2003. Polycystins 1 and 2 mediate mechanosensation in the primary cilium of kidney cells. *Nat. Genet.* 33:129–137. doi:10.1038/ng1076

Ogawa, H., N. Ohta, W. Moon, and F. Matsuzaki. 2009. Protein phosphatase 2A negatively regulates aPKC signaling by modulating phosphorylation of Par-6 in *Drosophila* neuroblast asymmetric divisions. *J. Cell Sci.* 122:3242–3249. doi:10.1242/jcs.050955

O'Neill, G.M., and E.A. Golemis. 2001. Proteolysis of the docking protein HEF1 and implications for focal adhesion dynamics. *Mol. Cell. Biol.* 21:5094–5108. doi:10.1128/MCB.21.15.5094-5108.2001

Pan, J., Q. Wang, and W.J. Snell. 2004. An aurora kinase is essential for flagellar disassembly in *Chlamydomonas*. *Dev. Cell*. 6:445–451. doi:10.1016/S1534-5807(04)00064-4

Pan, J., Q. Wang, and W.J. Snell. 2005. Cilium-generated signaling and cilia-related disorders. *Lab. Invest.* 85:452–463. doi:10.1038/labinvest.3700253

Plotnikova, O.V., E.N. Pugacheva, R.L. Dunbrack, and E.A. Golemis. 2010. Rapid calcium-dependent activation of Aurora-A kinase. *Nat Commun*. 1:64. doi:10.1038/ncomms1061

Pugacheva, E.N., and E.A. Golemis. 2005. The focal adhesion scaffolding protein HEF1 regulates activation of the Aurora-A and Nek2 kinases at the centrosome. *Nat. Cell Biol.* 7:937–946. doi:10.1038/ncb1309

Pugacheva, E.N., and E.A. Golemis. 2006. HEF1-aurora A interactions: points of dialog between the cell cycle and cell attachment signaling networks. *Cell Cycle*. 5:384–391. doi:10.4161/cc.5.4.2439

Pugacheva, E.N., S.A. Jablonski, T.R. Hartman, E.P. Henske, and E.A. Golemis. 2007. HEF1-dependent Aurora A activation induces disassembly of the primary cilium. *Cell*. 129:1351–1363. doi:10.1016/j.cell.2007 .04.035

Qian, Q., L.W. Hunter, M. Li, M. Marin-Padilla, Y.S. Prakash, S. Somlo, P.C. Harris, V.E. Torres, and G.C. Sieck. 2003. Pkd2 haploinsufficiency alters intracellular calcium regulation in vascular smooth muscle cells. *Hum. Mol. Genet.* 12:1875–1880. doi:10.1093/hmg/ddg190

Roderick, H.L., and S.J. Cook. 2008. Ca2+ signalling checkpoints in cancer: remodelling Ca2+ for cancer cell proliferation and survival. *Nat. Rev. Cancer*. 8:361–375. doi:10.1038/nrc2374

Ryan, M.J., G. Johnson, J. Kirk, S.M. Fuerstenberg, R.A. Zager, and B. Torok-Storb. 1994. HK-2: an immortalized proximal tubule epithelial cell line from normal adult human kidney. *Kidney Int.* 45:48–57. doi:10.1038/ki.1994.6

Singh, M., L. Cowell, S. Seo, G. O'Neill, and E. Golemis. 2007. Molecular basis for HEF1/NEDD9/Cas-L action as a multifunctional co-ordinator of invasion, apoptosis and cell cycle. *Cell Biochem. Biophys.* 48:54–72. doi:10.1007/s12013-007-0036-3

Singh, M.K., D. Dadke, E. Nicolas, I.G. Serebriiskii, S. Apostolou, A. Canutescu, B.L. Egleston, and E.A. Golemis. 2008. A novel Cas family member, HEPL, regulates FAK and cell spreading. *Mol. Biol. Cell*. 19:1627–1636. doi:10.1091/mbc.E07-09-0953

Skobeleva, N., S. Menon, L. Weber, E.A. Golemis, and V. Khazak. 2007. In vitro and in vivo synergy of MCP compounds with mitogen-activated protein kinase pathway- and microtubule-targeting inhibitors. *Mol. Cancer Ther.* 6:898–906. doi:10.1158/1535-7163.MCT-06-0602

Sneppen, K., S. Krishna, and S. Semsey. 2010. Simplified models of biological networks. *Annu Rev Biophys*. 39:43–59. doi:10.1146/annurev .biophys.093008.131241

Soncini, C., P. Carpinelli, L. Gianellini, D. Fancelli, P. Vianello, L. Rusconi, P. Storici, P. Zugnoni, E. Pesenti, V. Croci, et al. 2006. PHA-680632, a novel Aurora kinase inhibitor with potent antitumoral activity. *Clin. Cancer Res.* 12:4080–4089. doi:10.1158/1078-0432.CCR-05-1964

Streets, A.J., D.J. Moon, M.E. Kane, T. Obara, and A.C. Ong. 2006. Identification of an N-terminal glycogen synthase kinase 3 phosphorylation site which regulates the functional localization of polycystin-2 in vivo and in vitro. *Hum. Mol. Genet.* 15:1465–1473. doi:10.1093/hmg/ddl070

Streets, A.J., A.J. Needham, S.K. Gill, and A.C. Ong. 2010. Protein kinase D-mediated phosphorylation of polycystin-2 (TRPP2) is essential for its effects on cell growth and calcium channel activity. *Mol. Biol. Cell*. 21:3853–3865. doi:10.1091/mbc.E10-04-0377

Sweeney, W.E. Jr., R.O. von Vigier, P. Frost, and E.D. Avner. 2008. Src inhibition ameliorates polycystic kidney disease. *J. Am. Soc. Nephrol.* 19:1331–1341. doi:10.1681/ASN.2007060665

Tanaka, T., M. Kimura, K. Matsunaga, D. Fukada, H. Mori, and Y. Okano. 1999. Centrosomal kinase AIK1 is overexpressed in invasive ductal carcinoma of the breast. *Cancer Res.* 59:2041–2044.

Tanner, M.M., S. Grenman, A. Koul, O. Johannsson, P. Meltzer, T. Pejovic, A. Borg, and J.J. Isola. 2000. Frequent amplification of chromosomal region 20q12-q13 in ovarian cancer. *Clin. Cancer Res.* 6:1833–1839.

Tatsuka, M., H. Katayama, T. Ota, T. Tanaka, S. Odashima, F. Suzuki, and Y. Terada. 1998. Multinuclearity and increased ploidy caused by overexpression of the aurora- and Ipl1-like midbody-associated protein mitotic kinase in human cancer cells. *Cancer Res.* 58:4811–4816.

Wilson, P.D. 2004. Polycystic kidney disease. *N. Engl. J. Med.* 350:151–164. doi:10.1056/NEJMra022161

Wong, S.Y., A.D. Seol, P.L. So, A.N. Ermilov, C.K. Bichakjian, E.H. Epstein Jr., A.A. Dlugosz, and J.F. Reiter. 2009. Primary cilia can both mediate and suppress Hedgehog pathway-dependent tumorigenesis. *Nat. Med.* 15:1055–1061. doi:10.1038/nm.2011

Wu, J.C., T.Y. Chen, C.T. Yu, S.J. Tsai, J.M. Hsu, M.J. Tang, C.K. Chou, W.J. Lin, C.J. Yuan, and C.Y. Huang. 2005. Identification of V23RalA-Ser194 as a critical mediator for Aurora-A-induced cellular motility and transformation by small pool expression screening. *J. Biol. Chem.* 280:9013–9022. doi:10.1074/jbc.M411068200

Xu, J., H. Li, B. Wang, Y. Xu, J. Yang, X. Zhang, S.K. Harten, D. Shukla, P.H. Maxwell, D. Pei, and M.A. Esteban. 2010. VHL inactivation induces HEF1 and Aurora kinase A. *J. Am. Soc. Nephrol.* 21:2041–2046. doi:10.1681/ASN.2010040345

Yamada, M., S. Hirotsune, and A. Wynshaw-Boris. 2010. The essential role of LIS1, NDEL1 and Aurora-A in polarity formation and microtubule organization during neurogensis. *Cell Adh Migr*. 4:180–184. doi:10.4161/cam.4.2.10715

Zhang, D., T. Hirota, T. Marumoto, M. Shimizu, N. Kunitoku, T. Sasayama, Y. Arima, L. Feng, M. Suzuki, M. Takeya, and H. Saya. 2004. Cre-loxP-controlled periodic Aurora-A overexpression induces mitotic abnormalities and hyperplasia in mammary glands of mouse models. *Oncogene*. 23:8720–8730. doi:10.1038/sj.onc.1208153

Zhou, H., J. Kuang, L. Zhong, W.L. Kuo, J.W. Gray, A. Sahin, B.R. Brinkley, and S. Sen. 1998. Tumour amplified kinase STK15/BTAK induces centrosome amplification, aneuploidy and transformation. *Nat. Genet.* 20:189–193. doi:10.1038/2496